Characterization of Activated Carbon Prepared From the Nucleus of Ziziphus Lotus (NBEG): Isothermal Study and Kinetics of Adsorption of Methylene Blue

Ibrahim Touzani
Universite Sidi Mohamed Ben Abdellah Faculte des Sciences et Techniques de Fes
Kawtar FIKRI-BENBRAHIM (kawtar.fikribenbrahim@usmba.ac.ma)
Universite Sidi Mohamed Ben Abdellah Faculte des Sciences et Techniques de Fes
https://orcid.org/0000-0002-2923-9299
Hammou Ahlafi
Universite Moulay Ismail Faculte des Sciences
Bouchaib Ihssane
Sidi Mohamed Ben Abdellah University Faculty of Science and Technology of Fez: Universite Sidi Mohamed Ben Abdellah Faculte des Sciences et Techniques de Fes
Otmane Boudouch
Universite Sultan Moulay Slimane Faculte des Sciences et Techniques

Research Article

Keywords: chemical activation, adsorption, kinetics, methylene blue, activated carbon, isotherm, Nbeg Ziziphus lotus cores

Posted Date: June 17th, 2021

DOI: https://doi.org/10.21203/rs.3.rs-619904/v1

CHARACTERIZATION OF ACTIVATED CARBON PREPARED FROM THE NUCLEUS OF *ZIZIPHUS LOTUS* (NBEG): ISOTHERMAL STUDY AND KINETICS OF ADSORPTION OF METHYLENE BLUE

Ibrahim Touzani[1,2], Kawtar Fikri-Benbrahim[1*], Hammou Ahlafi[3], Bouchaib Ihssane[4] and Otmane Boudouch[5]

[1] Laboratory of Microbial Biotechnology and Bioactive Molecules, Sciences and Technologies Faculty, Sidi Mohamed Ben Abdellah University, P.O. Box 2202, Fez, Morocco.

[2] High Institute of Nursing Professions and Health Techniques annex Taza, Fez, Morocco.

[3] Laboratory of Chemistry and Biology Applied to the Environment, Faculty of Sciences; Moulay Ismail University. P. O. Box. 11201 Zitoune, Meknès, 50060, Morocco.

[4] Laboratory of Applied organic Chemistry. Sciences and Technologies Faculty, Sidi Mohamed Ben Abdellah University, P.O. Box 2202, Fez, Morocco.

[5] Environmental & Agro-Industrial Processes team, Sciences and Technologies Faculty, Sultan Moulay Slimane University, P. O. Box 523, Beni-Mellal, Morocco.

[*] Corresponding author : Kawtar FIKRI-BENBRAHIM, *Laboratory of Microbial Biotechnology and Bioactive molecules, Sciences and Technologies Faculty, Sidi Mohamed Ben Abdellah University, P. O. Box 2202 Imouzzer Road, Fez, Morocco*

Tel : +212661216598 , kawtar.fikribenbrahim@usmba.ac.ma

Abstract

Ziziphus lotus (Nbeg) is very common in Morocco where it occupies various ecosystems and presents different interests; however it remains devalued and knows recent deterioration due to the human pressure through clearing, wood collection, irrational cuts' exploitation and overgrazing. This study aims to prepare activated carbon from the cores of this interesting biomaterial, for the first time to the best of our knowledge, according to a manufacturing process based on its chemical and thermal activation. The cores of *Ziziphus lotus* (Nbeg) were chemically activated by sulfuric acid (H_2SO_4, 98%) for 24h with a mass contribution (1:1), and then carbonized at a temperature of 500 °C for 2 hours. The obtained activated carbon was characterized by scanning electron microscopy, X-ray diffraction, Fourier transform infrared spectroscopy and specific surface measurement. These characterization results showed an important porosity and a surface structure having acid groups and carboxylic functions. The adsorption of methylene blue (MB) was evaluated, by Langmuir and Freundlich models examination, in order to explain the adsorption efficiency in a systematic and scientific way. Also pseudo-first order and pseudo-second order kinetic models were used to identify the possible mechanisms of this adsorption process. The results showed that the MB adsorption process on activated carbon follows the Langmuir model and that the adsorption kinetic is best represented by kinetics data of the pseudo-second order model. Therefore, *Z. lotus* can be used as a low-cost available material to prepare a high quality activated carbon having a promising potential in the wastewater treatment.

Keywords: chemical activation, adsorption, kinetics, methylene blue, activated carbon, isotherm, Nbeg *Ziziphus lotus* cores.

Introduction

Water is the most fundamental and essential element of all natural resources. Its role is crucial for the economic and social development of a country; nevertheless the management of water resources is a challenge for most countries in the world. Currently, these resources are facing problems of quantity and quality, related to global warming and irrational use. Thus, their quality is increasingly worsened by various pollutant discharges, such as urban and industrial wastewaters (Touzani et al., 2020), leading to pollution of surface water, groundwater and soil, which can directly affect ecosystems and the services they provide (Corcoran, 2010).

Waste-water can contain many substances, in solid or dissolved forms that are more or less biodegradable (Alsheyab et al., 2018). Among these organic micro-pollutants, dyes are used in many industrial sectors such as textiles, food and cosmetics. Dyes have characteristics of synthetic origin and a complex molecular structure that makes them more stable and difficult to biodegrade (Ghaedi et al., 2014). The various dyes that exist in industrial effluents can present adverse environmental effects, as they cause a change in the color of waters, reducing sunlight penetration and photosynthetic activities (Sikdar et al., 2020). As a result, ecological damage can spread downstream to agricultural or aquaculture areas, affecting aquatic flora and fauna (Abbas and Trari, 2020). In addition, they can also cause eye burns responsible for permanent injury to human and animal eyes, or waterborne diseases which could be are considered carcinogenic and dangerous even at trace amounts (Mansour et al., 2011).

The treatment of industrial effluents containing different types of dyes is found to be of great interest to preserve our environment. Various methods of wastewater purification and treatment have been developed and used, including coagulation, ozonation, precipitation, flocculation and adsorption (Abbas et al., 2019). The latter is the most widely used method because it has very significant technical, economic, and environmental advantages (Bagheri et

al., 2016). In addition, it is universal as it can be used to remove soluble, insoluble, and biological contaminants with 90-99% removal efficiency compared to other treatment methods.

Since the introduction of this process, activated carbon has been one of the most frequently used products due to its highly developed adsorption capacity. The main characteristics of activated carbon are its porous structure, in relation linked to the accessible specific surface area into which molecules can penetrate, the pore size distribution and their average geometric shape (Li et al., 2020). The adsorption properties of activated carbon depend on the functional groups, resulting mainly from the activation process, on the precursors, and thermal purification (Yousefi et al. 2019). Therefore, the selection of activation agents remains a key issue for many researchers. Thus, several scientific papers report activation with potassium hydroxide (Wang et al., 2015; Abbas and Ahmed 2016), phosphoric acid (Kyzas et al., 2016; Han et al., 2020), zinc chloride (Erdem et al., 2016; Spagnoli et al., 2017), and new activation agents (Heidarinejad et al., 2020). In addition, many authors have investigated the efficiency of inexpensive and available substances for the synthesis of activated carbon (Liu et al., 2019). This has led to a growing interest in the production of activated carbon from renewable and low-cost precursors from agricultural waste. The most common activation sources on a commercial scale are wood, anthracite, bitumen charcoal, lignite, coconut shell, and almond shells. Today, much effort is devoted to the exploitation of industrial waste and agricultural residues as raw materials for coal production. Among its products are walnut shells (Yang and Qiu, 2010), argan shells (Elmouwahidi, et al., 2012), snail shell (Gumus and Okpeku, 2014), olive nibs (Moubarik and Grimi, 2015), potato peel (Guechi et al. 2016), sugar cane bagasse (Azmi et al., 2016), date press cake (Heidarinejad et al., 2018), betel nuts (Cundari et al., 2018) and prickly pear seeds (El Maguana et al., 2019).

This study concerns the preparation of an activated carbon from a biomaterial and its manufacturing process based on chemical and thermal activation. The biomaterial used in this study is the cores of *Ziziphus lotus* (Nbeg). The latter is very abundant and occupies various geographical areas of Morocco (Benabid, 2000). Indeed, *Ziziphus lotus* is a species present in several biotopes of arid and semi-arid regions. It grows on all soils: limestone, siliceous, clayey and sandy (Ionesco and Sauvage, 1969). Another part of this study concerns the use of this activated carbon as a new support for the depollution of urban and industrial wastewater loaded with organic pollutants such as dyes. In this framework, an example of adsorption of methylene blue CI 52015 is evaluated and its kinetic models are used to identify possible mechanisms of adsorption processes. Langmuir and Freundlich models are examined to explain the adsorption efficiency in a systematic and scientific manner.

Materials and methods

Preparation of activated carbon

The preparation of our activated carbon follows several steps. The fruits of Nbeg: *Ziziphus lotus* wild (NZL) were harvested at full maturity in September 2018 in the region of Taza (Morocco). These fruits are characterized by a brown color and round shape; the kernels have an elongated shape, a light color and a rough texture. The NZL pits were washed several times and then dried in the shade and protected from dust, before being ground into fine particles. Chemical activation of NZL was carried out by sulfuric acid (H_2SO_4, 98%) for 24h with mass contribution (1:1). Then, the resulting paste was washed with distilled water until the pH of the washing solution reached a neutral value, and then dried at 100 °C for four hours. Then, the dried paste was carbonized at a temperature of 500 °C for two hours. The resulting activated carbon was ground into small particles of sizes less than 100 µm and named CNZL. The characterization of CNZL was performed using different analytical

techniques: Scanning electron microscopy (SEM) identified by Quanta 200 model SEM equipped with a tungsten filament electron gun; X-ray diffraction (XRD) performed by XPERT-PRO type XRD in a scan area ranging from 5 to 120° 2θ. Fourier transform infrared spectroscopy (FTIR) was performed in the mid-infrared region using a Vertex 70 spectrometer. Specific surface area and pore structure were determined using an ASAP Micromeritics apparatus by adsorption of liquid nitrogen N_2 at T = -196 °C using the Brunauer-Emmet-Teller (BET) method and the Barrett-Joyner-Halenda (BJH) method.

Adsorption of CI 52015 dye

Adsorbate preparation

The pollutant considered in our study is the methylene blue (MB) dye CI 52015. Figure 1, shows the developed chemical structure of MB, while Table 1 groups its main physical properties. Solutions of different concentrations of 20, 30 and 40 mg/L were obtained by diluting a stock solution of MB (at 5g/L) with distilled water.

Figure 1. Molecular structure of Methylene blue (CI 52015)

Table 1. Physical Properties and Molecular Structure of Methylene blue: CI 52015

Name of dye	Methylene Blue
Color index number	52015
CAS Number	61-73-4
Chemical Formula	$C_{16}H_{18}N_8SCl$
Molecular weight (g/L)	390.2 (cm3/g mol)
Λmax	662.5 nm
Solubility in water	1 g/25 mL

Effect of contact time

The contact time is one of the most important factors during chemical reactions. Hence, the effect of contact time on the removal rate of MB, was studied for a time interval of 10-120 min for each initial concentration (20, 30 and 40 mg/L), in the presence of 0.1g CNZL activated carbon at room temperature. So, in closed reactors, 100 ml of each methylene blue concentration was put in contact with 0.1g of CNZL activated carbon under stirring at 300rpm. Every 10 min, the mixture was centrifuged at 5000rpm for 5 min, and then the concentrations of MB in the supernatants were measured at 665 nm using an UV-Visible spectrometer.

The abatement rate R (%) was calculated from the following equation:

$$R(\%) = \frac{C_0 - C_e}{C_0} \times 100$$

Where C_0 (mg/L) is the initial concentration of MB and C_e (mg/L) is the concentration of MB in solution.

155 **Kinetics of adsorption**

156 Kinetics provides information about the adsorption mechanism and the mode of transfer of
157 solutes from the liquid to the solid phase. Hence, simplified kinetic models are adopted to
158 provide information about the adsorption mechanism. These models are generally well fitted
159 by two classical kinetic models, a pseudo-first order kinetic model (Damiyine et al., 2017) and
160 a pseudo-second order kinetic model (Fayoud et al., 2015). These two models were tested to
161 investigate the adsorption kinetics of methylene blue on CNZL activated carbon.

162 **Pseudo-first order**

163 This model is defined by the relationship below (Das et al., 2013):

164 $$\log\ (q_e - q_t) = \log q_e - \frac{K_1.t}{2.303}$$

165 Where q_e and q_t are the quantities of adsorbed ion ($mg.g^{-1}$) at equilibrium and time t,
166 respectively, and k_1 is the equilibrium velocity constant of pseudo first order (min^{-1}).

167 **Pseudo-second order**

168 This model is defined in the form below (Raoul et al., 2014).

169 $$\frac{t}{q_t} = \frac{1}{K_2 q_e^2} + \frac{t}{q_e}$$

170 Where k_2 is the pseudo-second order adsorption rate constant (g/mg.min).

171 **Adsorption isotherms**

172 An adsorption process can be described using an adsorption isotherm. Langmuir and
173 Freundlich isotherms are used as models to study the adsorption of MB on CNZL activated

carbon. An isotherm is a curve that represents the relationship between the amount of solute adsorbed per unit mass of adsorbent qe and the concentration of solute in solution Ce.

The amount of solute adsorbed is calculated using the equation (Ojemaye et al., 2017):

$$\mathbf{q_e} = \frac{(\mathbf{C_0} - \mathbf{C_e}).\mathbf{V}}{\mathbf{m}}$$

Where qe: equilibrium amount of solute adsorbed per unit weight of adsorbent (mg/g) ;

C_0: initial solute concentration (mg/L);

Ce: equilibrium solute concentration (mg/L);

m: mass of adsorbent (g);

V: volume of solution (L).

Langmuir model (Langmuir, 1918) is described mathematically by the following equation:

$$q_e = \frac{q_{max}\, K_L\, Ce}{1 + K_L C_e}$$

This equation is often written in linear form (Ali et al., 2016):

$$\frac{C_e}{q_e} = \frac{1}{K_L q_{max}} + \frac{1}{q_{max}} C_e$$

Where qe and qmax are respectively the equilibrium adsorption capacity and the maximum adsorption capacity (mg/g), K_L the characteristic constant of Langmuir, it is the equilibrium solution adsorbate concentration per unit mass of solid (mg/L).

Freundlich model (Freundlich, 1906) is described by the following empirical equation:

$$q_e = K_f * C_e^{\frac{1}{n}}$$

It can be expressed in logarithmic form according to Nourmoradi et al. (2016)

193 $$\log q_e = \log k_f + \frac{1}{n} \log C_e$$

194 Where :

195 qe is the amount of adsorbate material adsorbed per unit mass of adsorbent at equilibrium
196 (mg/g). This is the equilibrium concentration (mg/L),
197 K_f and n are respectively the adsorbent adsorption capacity and the adsorbent-adsorbate
198 sorption intensity.

199 **Results and discussions**

200 **Scanning Electron Microscopy (SEM)**

201 The purpose of the SEM examination is to illustrate the morphology and external porosity of
202 the activated carbon. A developed porosity allows increasing makes it possible to increase the
203 specific surface of the carbon and therefore the number of active sites on which the MB
204 molecules can eventually bind. Figure 2, shows a very porous morphology of CNZL activated
205 carbon with pores of different sizes ranging from 10 to 45µm and different shapes.

206 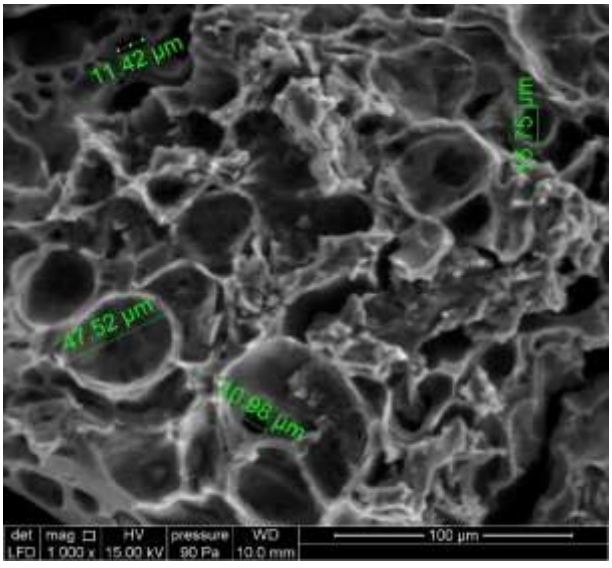

207 Figure 2. Image of the CNZL observed by Scanning Electron Microscopy (SEM).

X-ray Diffraction (XRD)

XRD is used to identify the crystalline or amorphous structure the CNZL. Figure 3, of the X-ray diffraction (XRD) shows very broad diffraction peaks, with a broad peak at approximately 2θ =25° indicating the presence of carbon. Thus, the absence of a sharp peak reveals a predominantly amorphous structure (Okman et al., 2014). Furthermore, there are noise signals consistent with the ash powder of the activated carbon.

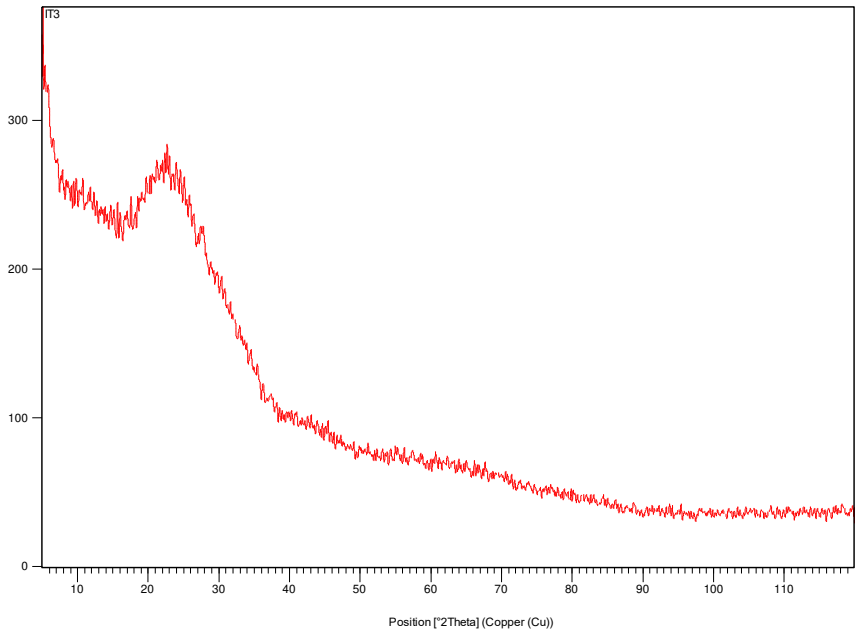

Figure 3. X-ray diffraction of the CNZL

Fourier transform infrared spectroscopy (FTIR)

Infrared spectroscopy is an analytical technique that is related to the vibrational properties of interatomic bonds; it can identify functional groups present in molecules. The infrared spectrum of CNZL illustrated in Figure 4 shows many functions on the surface of activated carbon, similar to those found in lingo-cellulosic materials (Abdel-Ghani et al., 2016).

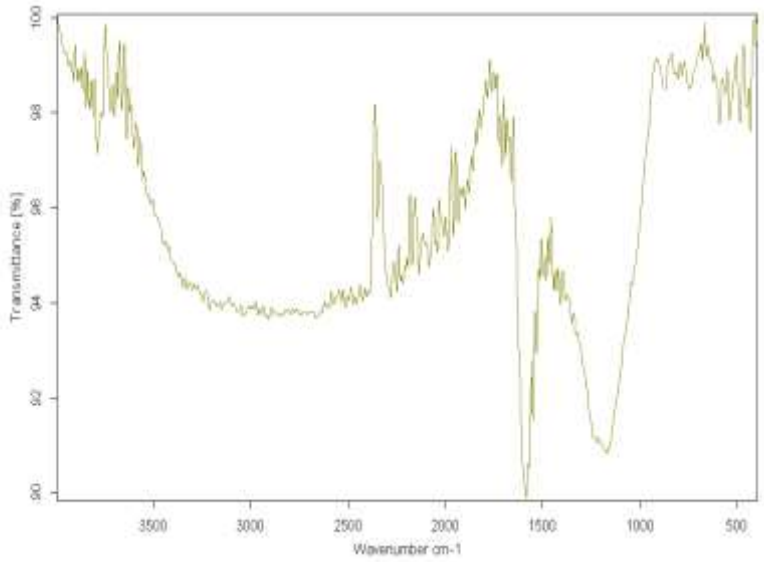

Figure 4. FTIR Spectrum of the CNZL

The adsorption bands are variable and narrow. The bands observed between 3700-3600 cm^{-1} correspond to the elongation vibrations of the free O-H bond of the alcoholic and phenolic groups; and the peak at 3640 cm^{-1} is attributed to the existence of free hydroxides. The bands between 3305-3200 cm^{-1} correspond to the hydrogen elongation vibrations of the hydroxyl groups and water. The bands observed between 2850 and 2930 cm^{-1} correspond to the symmetric and asymmetric valence vibration of the CH_2 bonds. The bands between 2200-2000 cm^{-1} correspond to the C≡C bond valence vibration of the alkyl function. The peak at 1680 cm^{-1} corresponds to the elongation vibration of C═C bonds in aromatic rings. A strong prominent band in the activated carbon appeared at 1575 cm^{-1} and corresponds to the presence of the carboxylic C=O groups on the surface. The bands observed in the 1400-1300 cm^{-1} region correspond to CH_2 deformation and/or O-H deformation vibrations supported by the existence of phenols. A broad band exists between 1200 -1100 cm^{-1} and corresponds to the valence vibration of C-O in the acid, alcohol and phenol groups, the peak at 1195 cm^{-1} is due to the S═O sulfur compounds present in the activated carbon. The band at 845 cm^{-1} as well as the bands that appear between 770-400 cm^{-1} represent vibrational distortion of C-H groups in aromatic rings.

Specific surface

The structure of an adsorbent is well defined by its specific surface area which represents the total surface area per unit mass of the product accessible to atoms and molecules, as well as the pore volume, the pore shape and the pore size distribution. Figure 5, shows a nitrogen adsorption/desorption isotherm obtained in the CNZL adsorbent. The adsorption curve obtained shows the characteristics of the type IV isotherm, where the surface of the adsorbent is completely covered by a monomolecular layer of N2 (B-point method), then beyond, several molecular layers (physisorption) are formed (according to the IUPAC classification) corresponding to mesoporous solids with capillary condensation. This is confirmed by the calculation of the pore size distribution, determined by the Barrett-Joyner-Halenda (BJH) method (Figure 6):

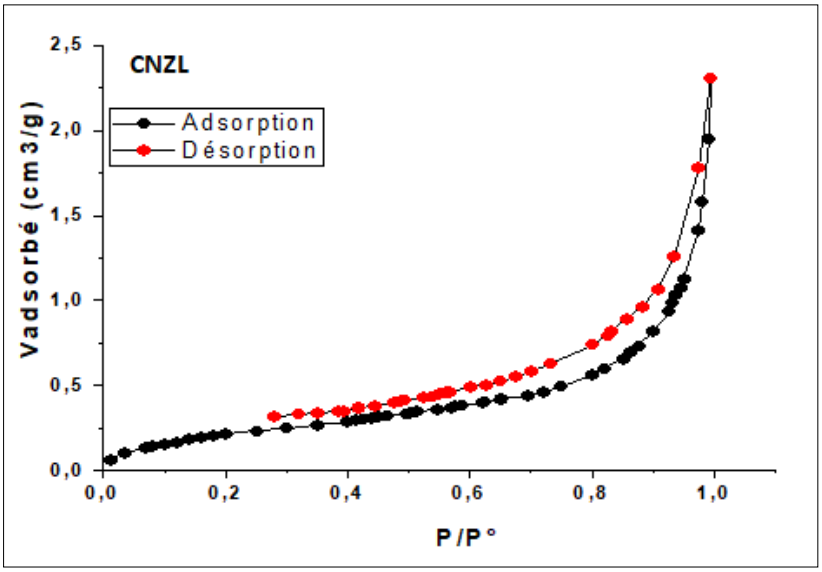

Figure 5. N2 adsorption/desorption isotherm of CNZL

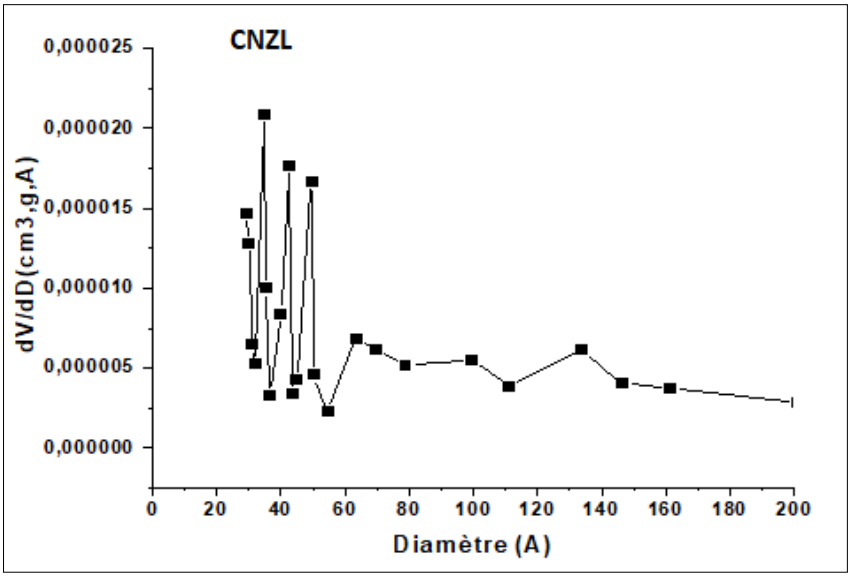

Figure 6. Pore diameter distribution of the CNZL

This pore distribution shows average diameters between 20 and 60Å. Moreover, the specific surface area determined using the BET method is 0.749 m²/g.

Effect of contact time

Contact time is one of the most important factors in chemical reactions. In the adsorption process, the increasing of the adsorbate concentration in the solution leads to the adsorbates' introduction into the internal pores of the adsorbent due to the concentration gradient (Yousefi et al. 2019). Figure 7, shows the removal rate of different concentrations of methylene blue (20, 30 and 40 mg/L) over time; by CNZL-activated carbon adsorption. Results show that the adsorption process is very fast and the removal efficiency of MB is improved by increasing the contact time and depending on initial concentration. Indeed, more than 80% of the dye used amount is adsorbed during the 20 min, which could be due to the external mass transfer that is fast. Therefore, the increase in contact time greatly increases the removal efficiency, and enables to reach equilibrium at about 80 min for the tested concentrations. This means that there is an internal mass transfer of the adsorbent, which generally corresponds to a diffusion phenomenon in the internal porosity.

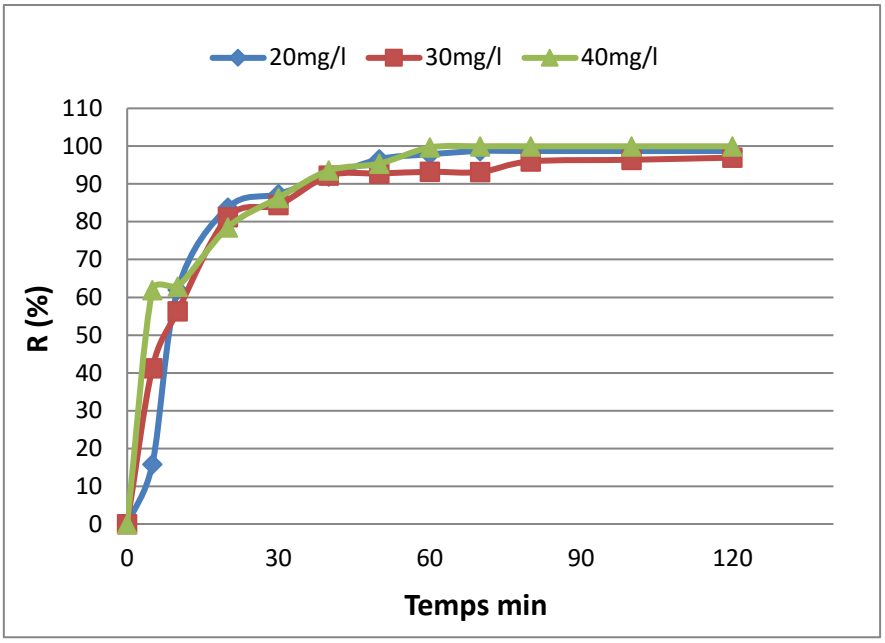

Figure 7. Removal rate of IC 52015 by CNZL

C= 20, 30, 40 mg/ l. m= 0.1g

Adsorption kinetics

The correlation coefficients as well as the kinetic constants corresponding to the two models used are determined by plotting the log (qe-qt) versus time (t) for the pseudo-first order model (Figure 8) and the (t/qt) versus time (t) for the pseudo-second order model (Figure 9). The parameters for the two models of the MB's adsorption at different initial concentrations on CNZL activated carbon are grouped in Table 2. These results reveal that the pseudo-first order R2 values are 0.954; 0.904 and 0.928 for MB concentrations of 20, 30 and 40 mg/L, respectively. As for the pseudo-second order R2 values are 0.999; 0.996 and 0.997 for MB concentrations of 20, 30 and 40 mg/L, respectively. This suggests that the kinetic data of MB adsorption on CNZL are better represented by the pseudo-second order model. Furthermore, values of the experimental adsorption capacity and those of the calculated adsorption capacity of the pseudo-second order model are very close, which reflects a good fit of this model to explain the adsorption process of MB on CNZL. Similarly it can be noticed that increasing the

initial MB concentration leads to a decrease in the value of the rate constant K2, which can be attributed to strong competition for sorption sites at high concentration leading to higher sorption rates (Abbas et al., 2016)..

Table 2. Adsorption kinetics parameters

		Pseudo-first order			Pseudo-second order		
	qe exp	qe,cal ($mg.g^{-1}$)	k1 (min^{-1})	R^2	qe,cal ($mg.g^{-1}$)	K2($g.mg^{-1}.min^{-1}$)	R^2
20 mg/L	4,935	3,411	0,064	0,954	5,23	0,037	0,999
30 mg/L	7,197	4,931	0,053	0,904	7,93	0,014	0,996
40 mg/L	9,996	12,05	0,062	0,928	10,86	0,009	0,997

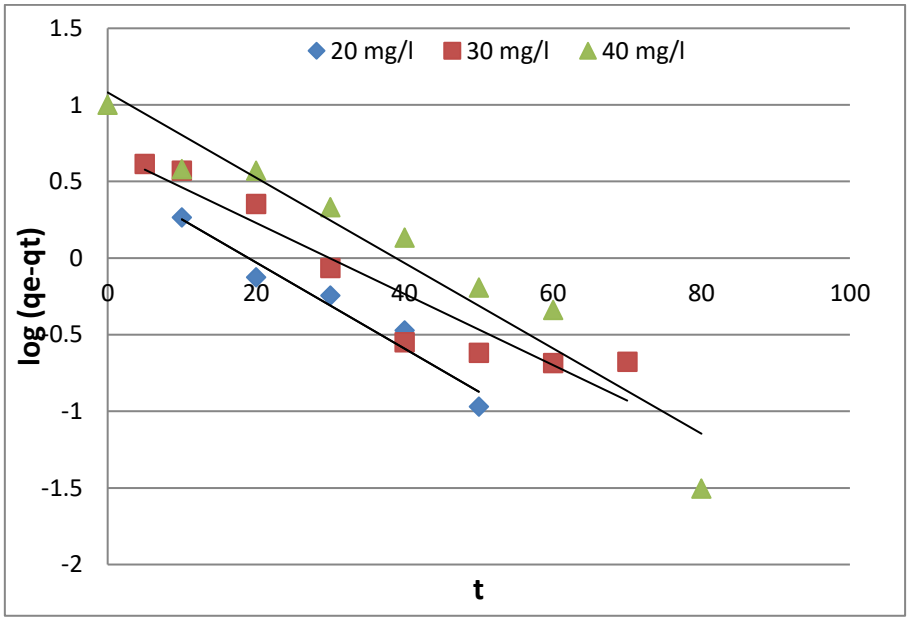

Figure 8. Pseudo-first order kinetic model

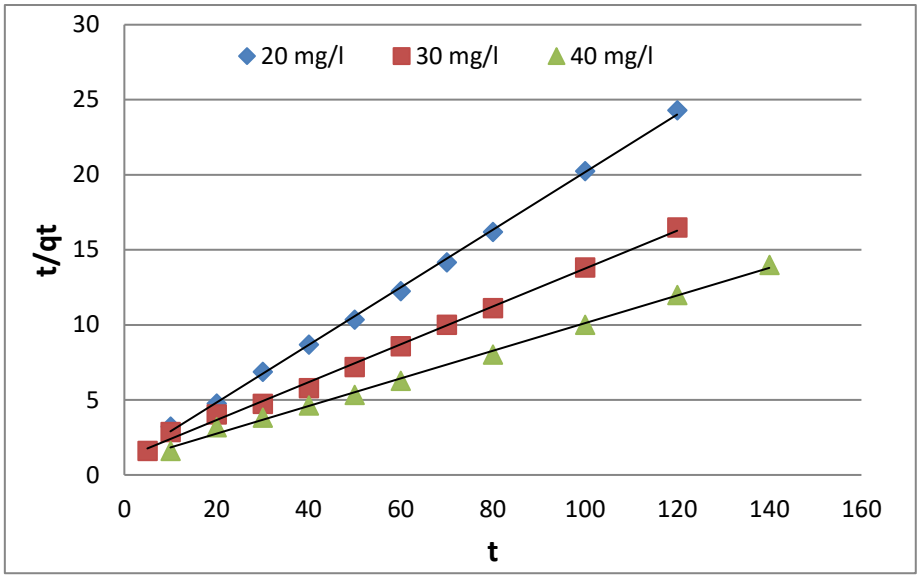

Figure 9. Pseudo-second order kinetic model

Adsorption isotherms

Adsorption isotherms are intended to describe how adsorbates interact with adsorbents, and are essential for optimizing the use of adsorbents (Tan et al., 2010). These isotherms allow us to determine the adsorption capacity and to highlight whether or not purification is feasible. To define the model to which the adsorption of MB is subjected, the experimental data have been applied to the equations of the two mathematical models of Langmuir and Freundlich. The Langmuir model is represented by the plot of Ce/qe versus Ce (Figure 10) and the Freundlich model is represented by the plot of log qe versus log ce (Figure 11), that give a linear graph with a slope of 1/n and the intercept with the x-axis give log Kf, from which n and Kf, respectively, can be calculated. Table 3 summarizes the results of both isotherms. These results show that the correlation coefficient R2 of the adsorption isotherm of the Langmuir model presents the highest value and is very close to unity compared to the Freundlich model, as well as the maximum adsorption capacity is 14.493 mg/g. This indicates that the adsorption process of the MB on CNZL follows the Langmuir model, and that the adsorption occurs in monolayer and involves independent identical sites in limited number (Yang et al., 2018).

Table 3. Parameters of the adsorption isotherm

	Langmuir			Frendlich		
	qmax (mg/g)	K_L(L/mg)	R2	KF (mg.g^{-1}) (L.mg^{-1})$^{1/n}$	1/n	R2
CNZL	14,493	1,500	0,982	6,45654229	0,926	0,899

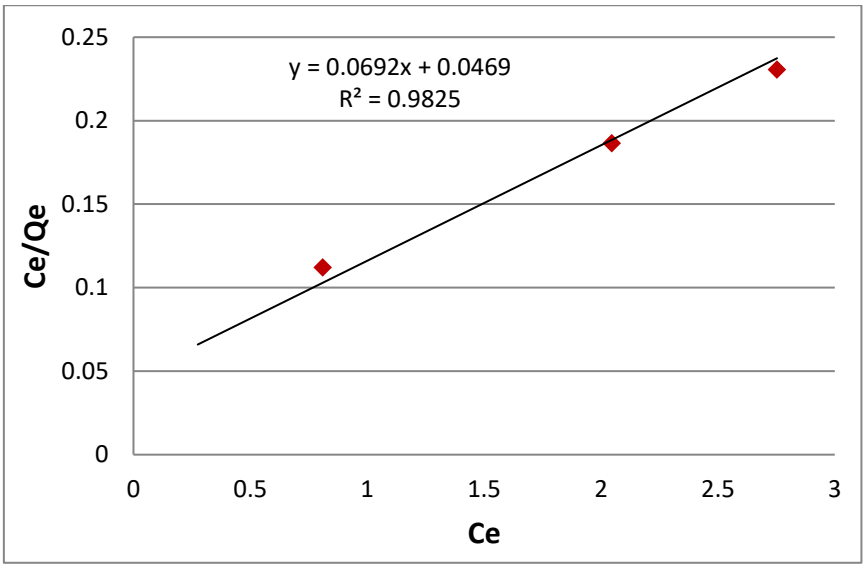

Figure 10. The Langmuir model representation

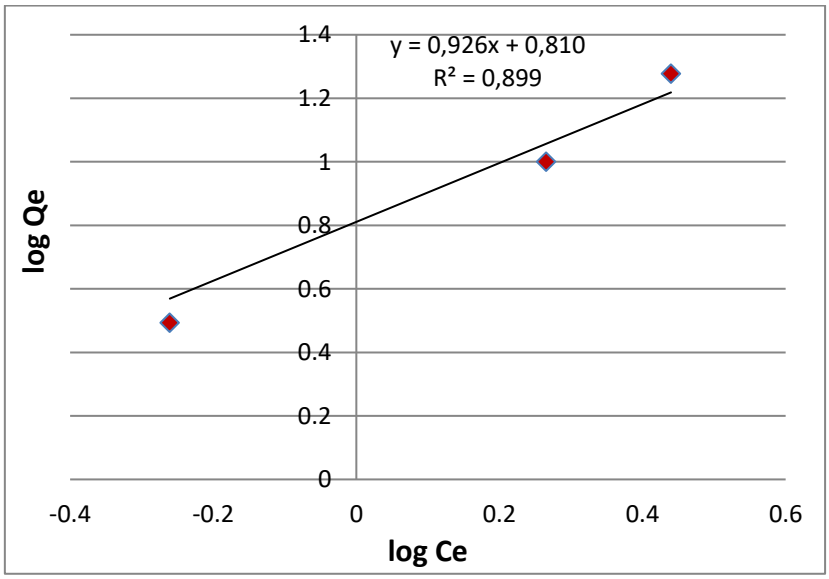

Figure 11. The Freundlich model representation

Conclusion

This study was carried out in order to prepare an activated carbon from a biomaterial by using a manufacturing process based on chemical and thermal activation. The results of this work show that the cores of *Ziziphus lotus* (Nbeg) represent an interesting source of raw material for the preparation of high quality activated carbon. The activated carbon was obtained using a chemical and thermal activation processes. The chemical activation was carried out by sulfuric acid (H_2SO_4, 98%) with a mass contribution (1:1), and the carbonization was conducted at a temperature of 500ºC for a duration of 2 h. Characterization results by scanning electron microscopy and Fourier transform infrared spectroscopy reveals the presence of a porous structure having different functions on the surface of CNZL. Moreover, results show that the adsorption process is very fast. The adsorption isotherm data are well fitted with the Langmuir monolayer model. Kinetic modeling of MB adsorption on CNZL activated carbon follows the pseudo-second order model well. Furthermore, these results proved that CNZL can be used as a new low-cost carrier for the remediation of urban and industrial waste-water loaded with organic pollutants such as dyes. Finally, this carbon should be promoted and considered as a cheaper alternative to commercial adsorbents.

Abbreviations

Nbeg: *Ziziphus lotus* (NZL), Scanning electron microscopy (SEM), X-ray diffraction (XRD), Fourier transform infrared spectroscopy (FTIR), Brunauer-Emmet-Teller (BET), Barrett-Joyner-Halenda (BJH), methylene blue (MB)

Declarations

Ethics approval and consent to participate

Not applicable.

Consent for publication

Not applicable.

Data Availability

All data generated or analyzed during the current study are available from the corresponding author on reasonable request.

Conflicts of interest

The authors declare that there is no conflict of interest.

Funding

Not applicable

Authors' contributions

IT: Contribution to study conception, conduction of methodology, writing of the manuscript.

KFB: Study’s design and supervising, correction and proofreading of the manuscript.

HA: Supervision of the specific surface part of the study.

BI: Contribution to the methylene blue absorption study.

OB: Conception of the study, Contribution to corrections.

All authors read and approved the final version.

Acknowledgements

The authors would like to express their sincere thanks to the director of the Innovation City of Sidi Mohamed Ben Abdellah University: Pr. S. Ibnsouda Koraichi; as well as to all the team of the platform of analyses, in particular Dr. H. El Knidri and Pr. M. Akhazzane. A special thank to Pr. A. Amin of the Faculty of Sciences of Meknes (Moulay Ismail University).

References

Abbas AF, Ahmed MJ (2016) Mesoporous activated carbon from date stones (Phoenix dactylifera L.) by one-step microwave assisted K2CO3 pyrolysis. J Water Process Eng, 9, 201-207. https://doi.org/10.1016/j.jwpe.2016.01.004

Abbas M, Harrache Z, Trari, M (2019) Removal of gentian violet in aqueous solution by activated carbon equilibrium, kinetics, and thermodynamic study. Adsorpt Sci Technol. 37(7-8):566-589. https://doi.org/10.1177/0263617419864504

Abbas M, Trari M (2020) Removal of methylene blue in aqueous solution by economic adsorbent derived from apricot stone activated carbon. Fibers Polym 21, 810–820. https://doi.org/10.1007/s12221-020-8630-8

Abdel-Ghani NT, El-Chaghaby GA, ElGammal MH, Rawash ESA (2016) Optimizing the preparation conditions of activated carbons from olive cake using KOH activation. New Carbon Mater. 31(5), 492-500. https://doi.org/10.1016/S1872-5805(16)60027-6

Ali RM, Hamad HA, Hussein MM, Malash GF (2016) Potential of using green adsorbent of heavy metal removal from aqueous solutions: adsorption kinetics, isotherm, thermodynamic, mechanism and economic analysis. Ecol Eng. 91, 317-332. https://doi.org/10.1016/j.ecoleng.2016.03.015

Alsheyab MAT, Kusch-Brandt S. Potential Recovery Assessment of the Embodied Resources in Qatar's Wastewater. Sustainability 2018; 10(9):3055. https://doi.org/10.3390/su10093055

Azmi NB, Bashir MJ, Sethupathi S, Ng CA (2016) Anaerobic stabilized landfill leachate treatment using chemically activated sugarcane bagasse activated carbon: kinetic and equilibrium study. Desalina Water Treat. 57:9, 3916-3927, https://doi.org/10.1080/19443994.2014.988660

386 Bagheri AR, Ghaedi M, Asfaram A, Hajati S, Ghaedi AM, Bazrafshan A, Rahimi MR (2016).
387 Modeling and optimization of simultaneous removal of ternary dyes onto copper sulfide
388 nanoparticles loaded on activated carbon using second-derivative spectrophotometry. J
389 Taiwan Inst Chem E. 65, 212-224. https://doi.org/10.1016/j.jtice.2016.05.004

390 Benabid A. (2000). Flore et écosystème du Maroc: évaluation et préservation de la
391 biodiversité. Ibis Press, Paris, 357 p.

392 Corcoran E. (Ed.) (2010) Sick water. the central role of wastewater management in
393 sustainable development: a rapid response assessment. UNEP/Earthprint.

394 Cundari L, Sari KF, Anggraini, L (2018) Characteristic of betel nuts activated carbon and its
395 application to Jumputan wastewater treatment. Mater Sci Eng, 345, 1-8.

396 Damiyine B, Guenbour A, Boussen R (2017) Adsorption of rhodamine B dye onto expanded
397 perlite from aqueous solution: kinetics, equilibrium and thermodynamics. J Mater Environ
398 Sci, 8, 345-355.

399 Das B, Mondal NK, Bhaumik R, Roy P, Pal KC, Das CR (2013) Removal of copper from
400 aqueous solution using alluvial soil of Indian origin: equilibrium, kinetic and thermodynamic
401 study. J Mater Environ. Sci, 4(4), 392-409.

402 El Maguana Y, Elhadiri N, Bouchdoug M, Benchanaa M, Jaouad A (2019) Activated carbon
403 from prickly pear seed cake: optimization of preparation conditions using experimental design
404 and its application in dye removal. Int J Chem Eng. 2019.
405 https://doi.org/10.1155/2019/8621951

406 Elmouwahidi A, Zapata-Benabithe Z, Carrasco-Marín F, Moreno-Castilla C (2012) Activated
407 carbons from KOH-activation of argan (Argania spinosa) seed shells as supercapacitor
408 electrodes. Bioresource technol. 111, 185-190.
409 https://doi.org/10.1016/j.biortech.2012.02.010

410 Erdem M, Orhan R, Şahin M, Aydın E (2016) Preparation and characterization of a novel
411 activated carbon from vine shoots by ZnCl 2 activation and investigation of its rifampicine
412 removal capability. Water Air Soil Poll. 227(7), 226. https://doi.org/10.1007/s11270-016-
413 2929-5

414 Fayoud N, Younssi SA, Tahiri S, Albizane A (2015) Kinetic and thermodynamic study of the
415 adsorption of methylene blue on wood ashes. J Mater Environ. Sci, 6(11), 3295-3306.

416 Freundlich HMF (1906) Over the adsorption in solution. J Phys Chem. 57(385471), 1100-
417 1107.

418 Ghaedi M, Ghazanfarkhani MD, Khodadoust S, Sohrabi N, Oftade M (2014) Acceleration of
419 methylene blue adsorption onto activated carbon prepared from dross licorice by ultrasonic:
420 Equilibrium, kinetic and thermodynamic studies. J Ind Eng Chem 20(4), 2548-2560.
421 https://doi.org/10.1016/j.jiec.2013.10.039

422 Guechi EK, Hamdaoui O (2016) Sorption of malachite green from aqueous solution by potato
423 peel: kinetics and equilibrium modeling using non-linear analysis method. Arab j chem, 9,
424 S416-S424. https://doi.org/10.1016/j.arabjc.2011.05.011

425 Gumus RH, Okpeku I (2014) Production of activated carbon and characterization from snail
426 shell waste (Helix pomatia). Adv Chem Eng Sci. 5, 51-61. DOI:10.4236/aces.2015.51006

427 Han Q, Wang J, Goodman BA, Xie J, Liu Z (2020) High adsorption of methylene blue by
428 activated carbon prepared from phosphoric acid treated eucalyptus residue. Powder Technol.
429 366, 239-248. https://doi.org/10.1016/j.powtec.2020.02.013

430 Heidarinejad Z, Dehghani MH, Heidari M, Javedan G, Ali I, Sillanpää M (2020) Methods for
431 preparation and activation of activated carbon: a review. Environ Chem Lett **18,** 393–415.
432 https://doi.org/10.1007/s10311-019-00955-0

433 Heidarinejad Z, Rahmanian O, Fazlzadeh M, Heidari M (2018) Enhancement of methylene
434 blue adsorption onto activated carbon prepared from Date Press Cake by low frequency
435 ultrasound. J Mol Liq, 264, 591-599. https://doi.org/10.1016/j.molliq.2018.05.100

436 Ionesco T, Sauvage C (1969) Fichier des espèces climax. *Al Awamia*, *32*, 105-124.

437 Kyzas GZ, Deliyanni EA, Matis KA (2016) Activated carbons produced by pyrolysis of waste
438 potato peels: Cobalt ions removal by adsorption. Colloid Surface A. 490, 74-83.
439 https://doi.org/10.1016/j.colsurfa.2015.11.038

440 Langmuir I (1918) The adsorption of gases on plane surfaces of glass, mica and platinum. J
441 Am Chem soc. 40(9), 1361-1403. https://doi.org/10.1021/ja02242a004

442 Li X, Qiu J, Hu Y, Ren X, He L, Zhao N, Zhao X (2020) Characterization and comparison of
443 walnut shells-based activated carbons and their adsorptive properties. Adsorpt Sci Technol.
444 38(9-10), 450-463. https://doi.org/10.1177/0263617420946524

445 Liu QX, Zhou YR, Wang M, Zhang Q, Ji T, Chen TY, Yu DC (2019) Adsorption of
446 methylene blue from aqueous solution onto viscose-based activated carbon fiber felts:
447 Kinetics and equilibrium studies. Adsorpt Sci Technol. 37(3-4), 312-332.
448 https://doi.org/10.1177/0263617419827437

449 Mansour H, Boughzala O, Barillier D, Chekir-Ghedira L, Mosrati R (2011) Les colorants
450 textiles sources de contamination de l'eau: CRIBLAGE de la toxicité et des méthodes de
451 traitement. Revue des sciences de l'eau / J Water Sci, 24(3), 209–238.
452 https://doi.org/10.7202/1006453

453 Moubarik A, Grimi N (2015) Valorization of olive stone and sugar cane bagasse by-products
454 as biosorbents for the removal of cadmium from aqueous solution. Food Res Int. 73, 169-175.
455 https://doi.org/10.1016/j.foodres.2014.07.050

Nourmoradi H, Avazpour M, Ghasemian N, Heidari M, Moradnejadi K, Khodarahmi F, Moghadam FM (2016) Surfactant modified montmorillonite as a low cost adsorbent for 4-chlorophenol: Equilibrium, kinetic and thermodynamic study. J Taiwan Inst Chem E. 59, 244-251. https://doi.org/10.1016/j.jtice.2015.07.030

Ojemaye MO, Okoh OO, Okoh AI (2017) Adsorption of Cu2+ from aqueous solution by a novel material; azomethine functionalized magnetic nanoparticles. Sep Purif Technol. 183, 204-215. https://doi.org/10.1016/j.seppur.2017.02.055

Okman I, Karagöz S, Tay T, Erdem M (2014) Activated carbons from grape seeds by chemical activation with potassium carbonate and potassium hydroxide. Appl Surf Sci. 293, 138-142. https://doi.org/10.1016/j.apsusc.2013.12.117

Raoul TTD, Gabche AS, Mbadcam KJ, Ndifor-Angwafor NG, Nsami NJ (2014) Kinetics and equilibrium studies of adsorption of phenol in aqueous solution onto activated carbon prepared from rice and coffee husks. Int J Eng Techn Res. 2, 166-173.

Sikdar D, Goswami S, Das P (2020) Activated carbonaceous materials from tea waste and its removal capacity of indigo carmine present in solution: synthesis, batch and optimization study. Sustain Environ Res 30**,** 30. https://doi.org/10.1186/s42834-020-00070-8

Spagnoli AA, Giannakoudakis DA, Bashkova S (2017) Adsorption of methylene blue on cashew nut shell based carbons activated with zinc chloride: the role of surface and structural parameters. J Mol Liq. 229, 465-471. https://doi.org/10.1016/j.molliq.2016.12.106

Tan IAW, Hameed BH (2010) Adsorption isotherms, kinetics, thermodynamics and desorption studies of basic dye on activated carbon derived from oil palm empty fruit bunch. JApSc.10(21), 2565-2571. 10.3923/jas.2010.2565.2571

478 Touzani I, Machkor M, Boudouch O, El Machrafi I, Flouchi R, Fikri-Benbrahim K (2020)
479 Environmental Impact Assessment of Taza City's Wastewater: Application through Principal
480 Component Analysis. Scientifica, 2020. https://doi.org/10.1155/2020/9168569

481 Wang YX, Ngo HH, Guo WS (2015) Preparation of a specific bamboo based activated carbon
482 and its application for ciprofloxacin removal. Sci Total Environ. 533, 32-39.
483 https://doi.org/10.1016/j.scitotenv.2015.06.087

484 Yang J, Qiu K (2010) Preparation of activated carbons from walnut shells via vacuum
485 chemical activation and their application for methylene blue removal. Chem Eng J. 165(1),
486 209-217. https://doi.org/10.1016/j.cej.2010.09.019

487 Yang X, Li F, Xia M, Luo F, Jiang Y (2018) Investigation on the micro-structure and
488 adsorption capacity of cellulosic biomass carbon based montmorillonite composite. Micropor
489 Mesopor Mat. 256, 18-24. https://doi.org/10.1016/j.micromeso.2017.07.052

490 Yousefi M, Arami SM, Takallo H, Hosseini M, Radfard M, Soleimani H, Mohammadi AA
491 (2019) Modification of pumice with HCl and NaOH enhancing its fluoride adsorption
492 capacity: kinetic and isotherm studies. Hum Ecol Risk Assess : An Int J. 25(6), 1508-1520.
493 https://doi.org/10.1080/10807039.2018.1469968

Supplementary Files

This is a list of supplementary files associated with this preprint. Click to download.

- GraphicalabstractCNZL.png